Evidence of Nonlinear Chain Stretching in the Rheology of Transient Networks

Y. Séréro, V. Jacobsen, and J.-F. Berret*

Unité Mixte de Recherche CNRS/Université de Montpellier II no. 5581, Groupe de Dynamique des Phases Condensées, F-34095 Montpellier Cedex 05, France

R. May

Institute Laue-Langevin, BP 156, F-38042 Grenoble Cedex 9, France

Received August 10, 1999; Revised Manuscript Received December 13, 1999

ABSTRACT: We report on telechelic associating polymers in aqueous solutions that self-assemble into starlike flowers in the dilute regime and develop a fully connected network of flowers above some threshold concentration ϕ^* (∼1 wt %). The peculiarity of these telechelics is that the end caps are partially fluorinated. Small-angle neutron scattering has been used to investigate the form and structure factors of the starlike aggregates, and linear rheology was performed in order to identify the viscoelastic features of the physically cross-linked network. Taking advantage of the long network relaxation times, we use step-strain experiments of amplitudes γ comprised between 0.01 and 3 to explore the nonlinear regime of shear deformations. In the linear regime, the stress relaxation function is well described by a stretched exponential of the form $G(t) = G_0 \exp(-(t/\tau_0)^\alpha)$, where G_0 is the elastic modulus, τ_0 the relaxation time, and α an exponent close to 1 ($\alpha \sim 0.8$). With increasing deformations ($\gamma > 0.4$), the elastic modulus is found to increase (strain hardening) while simultaneously the viscoelastic relaxation time decreases. The strain hardening is interpreted in terms of nonlinear stretching of the elastically active chains whereas the reduction of the relaxation time indicates that the chain breakage probability depends on the chain extensions (or end-to-end distances).

Introduction

A water-soluble associating polymer is a polymeric chain that has been chemically modified by the adjunct of hydrophobic species at one or several places along the backbone. If this modification takes place at both extremities, the associating polymer is a telechelic. There exists by now a challenge which is to understand the structure and rheology of transient networks made from these associating polymers.[1]

In aqueous solutions, telechelic polymers can self-assemble into noninteracting flowerlike micelles at low concentrations. From their local structure, the flowerlike micelles compare well to star polymers or to copolymeric micelles.[2,3] The hydrophobic end caps are forming the inner core (with almost no water molecule present) whereas the polymeric chains are looping back to the core. Recently, the form factor of flowerlike micelles has been established by small-angle neutron scattering,[4] and it confirms the analogy with star polymers. Above a threshold concentration ϕ^*, a three-dimensional network of flowers arises from the percolation of links. These links are polymeric chains with both end caps attached to two different and neighboring micelles. The most remarkable behavior of such a network is its viscoelasticity. Encountered in many different types of telechelics,[1,4,5−10] solutions above ϕ^* are viscoelastic and characterized by a rheological linear response close to that of a Maxwellian fluid. For a Maxwellian fluid, the stress relaxation function is decreasing monoexponentially and defined by two quantities: an elastic modulus G_0 and a viscoelastic relaxation time τ_0.

* Corresponding author. E-mail berret@gdpc.univ-montp2.fr.

Since Green and Tobolsky,[11] this Maxwellian linear behavior is described on the molecular level. It results from the equilibrium dynamics of connections and detachments of the hydrophobic end caps. As explained more recently by Tanaka and Edwards[12,13] (see also the approaches by Yamamoto[14] and Lodge[15]), the instantaneous elasticity G_0 is proportional to the cross-link density, i.e., the number of elastically active chains (bridges) per unit volume. The viscoelastic relaxation time τ_0 is related to the average lifetime of a connection,[11] which in turn depends on the breakage probability of a cross-link.

In contrast, the nonlinear regimes of shear flow and deformation are much less understood. It has been found in several systems[5,6,10,16] that the steady shear viscosity exhibits three flow regimes: Above a Newtonian plateau at low shear rates ($\dot\gamma\tau_0 \ll 1$), the viscosity increases first (shear thickening), passes through a maximum around $\dot\gamma\tau_0 \sim 1$, and then decreases drastically (shear thinning). The physical origin of the shear thickening and thinning effects is still a matter of debate. Some authors have suggested that the shear thickening could be due to the increase of the density of elastically active chains[10,17] whereas an alternative picture considers the non-Gaussian stretching behavior of the connecting chains under shear flow.[15,18,19]

To shed some light on the flow and deformation mechanisms involved in the nonlinear rheology of transient networks, we have undertaken a systematic investigation of telechelics in which the hydrophobic end caps are partially fluorinated. Here, we report on two telechelic solutions at concentrations $\phi = 0.5\%$ and $\phi = 4\%$, which are below and above the threshold ϕ^*, respectively ($\phi^* \sim 1\%$). Small-angle neutron scattering

10.1021/ma991349d CCC: $19.00
Published on Web 02/17/2000

measurements were performed in order to determine the microscopic length scales of the network: the size of the flowerlike micelles (radius of gyration) and the average distance between cross-links. Using step strain experiments of different amplitudes, the linear and nonlinear stress relaxation functions of the solution at $\phi = 4\%$ are investigated. In the nonlinear regime of deformation, we found that the instantaneous network elasticity is enhanced (strain hardening effect), whereas simultaneously the average lifetime of connections decreases. Both phenomena are interpreted in terms of non-Gaussian stretching of the elastically active chains.

Experimental Section

Perfluoroalkyl-modified poly(ethylene oxide) (PEO) of molecular weight $M_n = 10\,000$ g/mol with a well-defined structure has been synthesized by reacting PEO with a large excess of isophorone diisocyanate (IPDI) to produce isocyanato functional precursor. This first stage is followed by the reaction of the terminal isocyanato group with a perfluoroalkyl alcohol ($C_8F_{17}(CH_2)_{11}OH$).[9] Since a diisocyanate group is used as a spacer between the hydrophobic end caps and the PEO middle chain, these telechelics belong to the class of associating polymers noted HEUR (hydrophobically ethoxylate urethane). In the following, they will be termed F-HEUR. During the synthesis, polycondensation occurs which yields telechelic chains with twice the initial molecular weight in a ratio 80%/20%.[9] The zero-shear viscosity of aqueous F-HEUR solutions exhibits a drastic increase above a threshold concentration $\phi^* = 1\%$ (from 10 to 10^6 times the viscosity of water). This effect was attributed to the formation of a multiconnected transient network of flowerlike micelles.[4,9] It should be mentioned that the synthesis of F-HEUR has been recently improved.[20] This new synthesis yields F-HEUR telechelics as monodisperse as the original unmodified poly(ethylene oxide) with in addition a rate of functionalization better than 95%. In this case, the telechelics are water-soluble only with addition of a small amount of cationic or anionic surfactants. Qualitatively, the rheological behaviors of solutions obtained with the first and second synthesis, with or without surfactant, are identical.

Small-angle neutron scattering (SANS) experiments were performed at ambient temperature at the Laboratoire Léon Brillouin (beamline PACE) and at the Institute Laue-Langevin (beamline D22). Aqueous solutions were prepared in D_2O to enhance the scattering contrast at concentrations below and above the threshold, from $\phi = 0.1\%$ to 10%. The data shown in this paper were collected at $\phi = 0.5\%$ and $\phi = 4\%$ on D22 at distances sample-to-detector 2, 4, 11, and 18 m, so to cover a wave-vector range $4 \times 10^{-3} - 0.5$ Å^{-1} (with a neutron wavelength of 6 Å). The incoherent scattering background of both solutions was calculated from the D_2O spectrum and from the equivalent amount of hydrogen atoms present in the PEO chain and in the end caps. The scattering from the solvent is independent of the wave vector, at 0.0492 ± 0.008 cm^{-1}.

To correlate the SANS data and mechanical response, the linear and nonlinear stress relaxation functions were performed on the same F-HEUR solution that was investigated by SANS ($\phi = 4\%$). We used a strain-controlled rheometer (Rheometrics fluid spectrometer) equipped with a cone-and-plate configuration (angle 0.02 rad, radii 30 or 50 mm). In step-strain experiments, an initial deformation γ is applied to the sample, and the resulting stress

$$\sigma(t,\gamma) = \gamma G(t,\gamma) \tag{1}$$

is recorded as a function of time. In the linear regime of deformation, $G(t,\gamma)$ becomes γ-independent and is noted $G(t,\gamma<\gamma_{lin})$. γ_{lin} denotes here the limit between linear and nonlinear regimes. Measurements were carried out for strain amplitudes $\gamma = 0.01-3$ and temperatures ranging between $T = 7$ °C and $T = 35$ °C. The F-HEUR solution at $\phi = 0.5\%$ was not investigated in step-strain experiments since it is Newtonian.

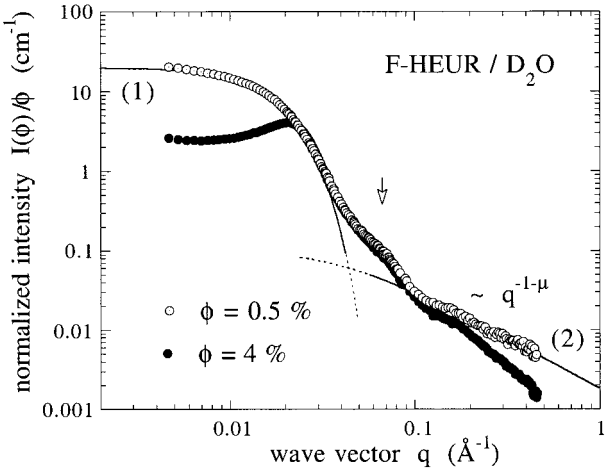

Figure 1. Neutron-scattered intensities of aqueous solutions of perfluoroalkyl telechelic polymers (F-HEUR) at concentration $\phi = 0.5\%$ and $\phi = 4\%$. The intensity has been normalized to the concentration ϕ. The continuous lines are the asymptotic behaviors derived from conventional star polymers (eq 1).[21] Note that for the solution at $\phi = 4\%$ the existence of a correlation peak and the good superposition with the data obtained at $\phi = 0.5\%$.

Experimental Results and Analysis

Small-Angle Neutron Scattering. Figure 1 shows the neutron scattering intensity $I(q,\phi)/\phi$ normalized to the concentration for F-HEUR solutions in the dilute and viscoelastic regimes, $\phi = 0.5\%$ and $\phi = 4\%$, respectively. For the $\phi = 0.5\%$, the absolute intensity saturates at low wave vectors at $I(q\rightarrow 0) = 10$ cm^{-1}. With increasing q, $I(q,\phi)/\phi$ strongly decreases but exhibits no marked oscillations. The main features of the solution at $\phi = 4\%$ are the existence of a correlation peak (at $q_{Max} = 0.026$ Å^{-1}) and a good superposition with the data obtained at $\phi = 0.5\%$ (in the range 0.03−0.1 Å^{-1}). Some deviations between both sets of data are visible at high wave vectors ($q > 0.1$ Å^{-1}).

a. Scattering Form Factor of Flowerlike Micelles. We now argue that the scattering function in the dilute regime is the form factor of noninteracting flowerlike micelles and can be approximated by the form factor of star polymers with large functionality f. Note that, in terms of aggregation number p, one has for telechelic flowers the relationship $2p = f$. In star polymers, simple analytical expressions for form factors are missing, but approximate expressions have been derived successfully. Following Grest et al.,[21] the scattered intensity reads

$$I(q,\phi\ll 1) = I(q\rightarrow 0)\exp\left(-\frac{q^2 R_G{}^2}{3}\right) + \beta\frac{\sin(\mu\tan^{-1}(q\xi))}{q\xi(1+q^2\xi^2)^{\mu/2}} \tag{2}$$

The first term on the right-hand side of eq 2 accounts for the overall size of the colloidal particle and determines its radius of gyration R_G (Guinier regime). This first term dominates at low q. The second term is the Fourrier transform of the monomer−monomer correlation function in the corona, in agreement with the monomer radial distribution obtained by Daoud et Cotton.[22] β is a prefactor depending of the functionality, ξ is the average blob size in the corona, and $\mu = 1/\nu - 1$ ($\nu = {}^3/_5$ in good solvent). Effective at large q, this second contribution decreases as $q^{-1/\nu}$. As shown in

Figure 1, the asymptotic scattering functions at low and high q are well explained by eq 1. Adjustable parameters are $I(q\rightarrow 0)$, R_G, β, ξ, and μ. We obtained a radius of gyration $R_G = 94$ Å and in the high-q region, power law exponents -1.3, and an average blob size $\xi = 30$ Å. An alternative model for the scattering form factor of block copolymer micelles has been proposed recently.[23] This model is based on the assumption of a Gaussian behavior of the polymeric chains forming the corona. A power law dependence of the scattered intensity is also predicted in the range $0.1-0.5$ Å^{-1}, but with an exponent of 2. It should be noticed that both approaches described above, as well as that of Adam and Lairez,[24] provide a qualitatively similar q dependence for the form factor.

The previous analysis deserves further comments:

(i) About the scaling law at large wave vectors, the disagreement with respect to the expected $q^{-5/3}$ of good solvent conditions should not be overestimated. In this q region, the scattered intensity is very sensitive to the incoherent background arising from the hydrogen atoms present in the medium (those of the PEO chains and hydrophobic end caps). According to standard analysis techniques used for SANS,[25] the incoherent scattering has to be subtracted to the raw data. At low ϕ and large q, however, both are of the same order. The incoherent background for a telechelic concentration ϕ is calculated from the measured spectrum of the solvent (D_2O) and from the number density of hydrogen atoms of the solution. For the two solutions investigated, we found $B_i(\phi = 0.5\%) = 0.0528$ cm^{-1} and $B_i(\phi = 4\%) = 0.0782$ cm^{-1}. However, due to the relatively low intensity obtained in the dilute regime, a variation of the background by 5% is sufficient to drop the exponent from -1.3 to ~ -2! The exponents at higher concentration are much more reliable and are around -2.

(ii) In the intermediate region, 0.05 Å^{-1} < q < 0.15 Å^{-1}, a bump is evidenced in the intensity that we ascribed to the core of the starlike micelles. From the smeared oscillations, we derived a crude estimate for the core radius, 35 ± 5 Å. Such a behavior has been already reported in copolymer micelles[26] and in stars of large functionality.[21]

(iii) The aggregation number p of the flowerlike micelles observed in Figure 1 can be derived from the extrapolated absolute intensity at $q \rightarrow 0$. In the dilute regime, $I(q\rightarrow 0,\phi)$ reads $n(\phi)(\overline{\Delta\rho})^2v^2$ where $n(\phi)$ is the number density of particles, $(\Delta\rho)$ the excess scattering length density of a telechelic with respect to D_2O, and v the dry volume of an aggregate. The parameter p enters the previous relationship in $n(\phi)$ as p^{-1} and in v^2 as p^2. Using $I(q\rightarrow 0) = 10$ cm^{-1}, we obtain an aggregation numbers $p = 49 \pm 6$ for the F-HEUR solution at $\phi = 0.5\%$.

b. Structure Factor of Flowerlike Micelles. With increasing ϕ, the neutron intensity of F-HEUR solutions scales with concentration (Figure 1, $q > 0.03$ Å^{-1}). This is a robust indication that the inner structure of self-assembled flowers remains unchanged in the ϕ range explored. This specific property, combined with the assumption of globular shape for the flowers, allows us to write the intensity as the product of a ϕ-independent form factor $P(q)$ and of a structure factor $S(q,\phi)$, according to

$$I(q,\phi) = n(\phi)\, P(q)\, S(q,\phi) \qquad (3)$$

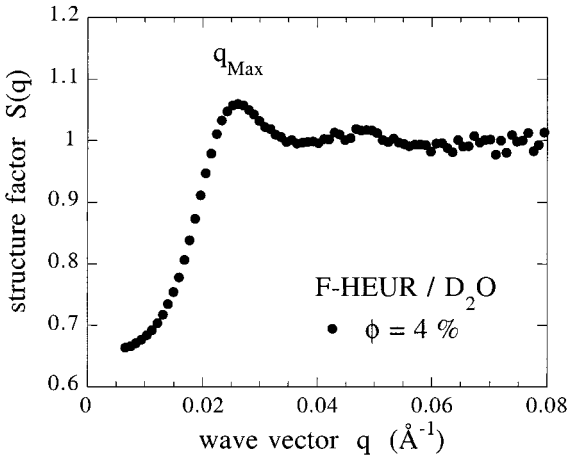

Figure 2. Experimental structure factor $S(q)$ for a F-HEUR solution at $\phi = 4\%$.

$S(q,\phi)$ accounts for the interactions between particles, and by definition it is 1 in the dilute regime. The static structure factor shown in Figure 2 for $\phi = 4\%$ is computed using eq 3. It is typical for dispersion of interacting colloidal particles. Note that in the network regime these interactions most probably comprise a repulsive contribution arising from spherical brushes and an attractive contribution due to bridging.[3,27] Assuming now that the first order at q_{Max} corresponds to the nearest-neighbor distances d of a locally face-centered-cubic (fcc) order, the particle density $n(\phi)$ can be calculated from geometrical considerations, according to

$$n(\phi) = q_{Max}{}^3/\pi^3\sqrt{108} \quad \text{using } d = \frac{\pi\sqrt{6}}{q_{Max}} \qquad (4)$$

The assumption of a local fcc packing (see also Alami et al.[28]) is further justified by the existence of a long-range order cubic phase above 10%. The maximum of the first order in $S(q,\phi = 4\%)$ at $q_{Max} = 0.0262$ Å^{-1} yields a density of flowers $n(\phi{=}4\%) = 5.6 \times 10^{16}$ cm^{-3} and an average distance $d = 300$ Å. These latter values are compatible with an aggregation number $p = 38 \pm 4$ at $\phi = 4\%$, in relative agreement with the analysis of the form factors in the dilute regime. A schematical representation of the flowerlike micelle made from perfluoroalkyl telechelics and deduced from the neutron data is shown in Figure 3.[21] These structural results are crucial for the interpretation of the rheological experiments discussed in the next section.

Rheology. a. Linear Response. The F-HEUR solution at $\phi = 4\%$ has been subjected to step-strain experiments at low deformation, yielding the stress relaxation function $G(t,\gamma<\gamma_{lin})$ characteristic of the linear regime (Figure 4). At short times and up to ~10 s, the mechanical response is rather constant and then decreases rapidly on the double-logarithmic scale. The initial stress developed in the sample is entirely relaxed within times ~500 s.

The linear viscoelastic response of F-HEUR network has been described at length in our previous reports,[4,9] and it will be reviewed here only briefly. It should be emphasized that the use of D_2O as solvent instead of H_2O as in our first investigations does not change qualitatively the results. In our former approaches, $G(t,\gamma<\gamma_{lin})$ was fitted at best by a stretched

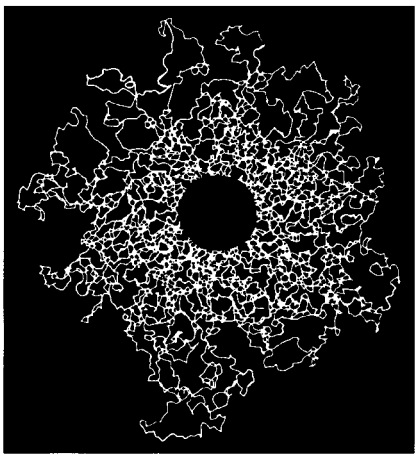

Figure 3. Schematical representation of the flowerlike micelles made from telechelic polymers with perfluoroalkyl hydrophobes. This image is inspired from the results of Monte Carlo simulations performed by Grest and co-workers on a 64-arm star polymer with 100 monomers per arm.[21] The length scales (radius, core) are deduced from the form factor obtained by small-angle neutron scattering.

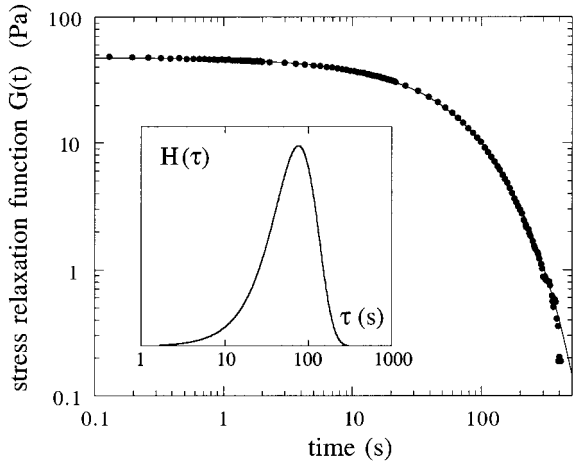

Figure 4. Stress relaxation function $G(t,\gamma<\gamma_{lin})$ as received from a step-strain experiment in the linear regime of deformation (F-HEUR/D_2O, $\phi = 4\%$, $T = 20$ °C). The continuous line through the data points is calculated according to eq 5 using $G_0 = 53 \pm 2$ Pa, $\tau_0 = 57 \pm 2$ s, and a stretched exponent $\alpha = 0.81 \pm 0.02$. The F-HEUR solution at $\phi = 4\%$ has a viscosity $\eta_0 = 3000$ Pa·s. Inset: distribution of relaxation times $H(\tau)$ associated with the relaxation modulus $G(t,\gamma<\gamma_{lin})$.

exponential of the form

$$G(t,\gamma<\gamma_{lin}) = G_0 \exp\left[-\left(\frac{t}{\tau_0}\right)^{\alpha}\right] \qquad (5)$$

Here, G_0 denotes the elastic modulus extrapolated as $t \rightarrow 0$, and τ_0 is the viscoelastic relaxation time in the linear regime. The continuous line in Figure 4 attests of quality of the fit. At $T = 20$ ° C, the linear viscoelastic parameters are $G_0 = 53 \pm 2$ Pa and $\tau_0 = 57 \pm 2$ s, with a stretched exponent $\alpha = 0.81 \pm 0.02$. For $\alpha \neq 1$, the zero-shear viscosity associated with the function in eq 2 reads $\eta_0 = G_0\tau_0\Gamma(\alpha)/\alpha$ where $\Gamma(\alpha)$ is the gamma function. Instead of the stretched exponential, the stress relaxation function can be described in terms of distribution of relaxation times, as well. This distribution (shown in the inset of Figure 4) is asymmetric, peaking around τ_0, and its width at half-maximum relates to the coefficient α. When the temperature is varied in the range $T = 7-35$ ° C, the form of the relaxation function $G(t,\gamma<\gamma_{lin})$ as provided by eq 2 remains the same.[9] In particular, the value of the stretched exponent $\alpha = 0.8$. However, the relaxation time τ_0 is found to decrease by 2 decades, from 450 to 4.5 s. In the Arrhenius plot of Figure 5, the straight line indicates a thermally activated dependence of the form $\tau_0(T) \propto \exp(E_A/k_BT)$, where k_B is the Boltzmann constant and E_A is the activation energy. The activation barrier associated with the data in Figure 5 is $E_A = 120$ kJ/mol, or when expressed in thermal energy units, $E_A = 48k_BT$ ($T = 300$ K). As mentioned by several authors,[13] the fact that the relaxation time is thermally activated indicates that the linear viscoelasticity is dominated by the activation process of the junction dissociation.

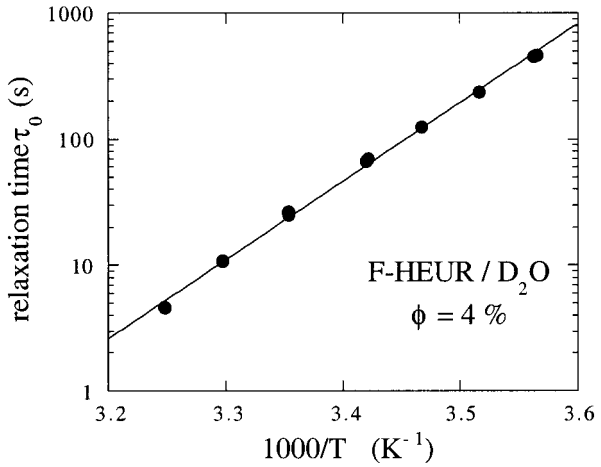

Figure 5. Viscoelastic relaxation time $\tau(T)$ versus inverse temperature for the F-HEUR/D_2O solution at $\phi = 4\%$. The straight line indicates a thermally activated process with an activation energy $E_A = 48k_BT$.

b. Nonlinear Response. For deformation amplitudes larger than γ_{lin}, the viscoelastic modulus $G(t,\gamma)$ depends on the applied strain. Figure 6 shows the stress relaxation function $G(t,\gamma)$ of the F-HEUR/D_2O solution at $\phi = 4\%$ for strain amplitudes ranging from 0.05 to 2.5 ($T = 20$ ° C). The low and high deformation ranges are considered separately, in Figure 6a for $\gamma = 0.05-2$ and in Figure 6b for $\gamma = 1.75-2.5$. Note in Figure 6b the use of the double-logarithmic scale. To allow comparisons, the relaxation functions in the linear regime, as well as for $\gamma = 1.75$ and $\gamma = 2$, are displayed in both figures.

The most noticeable result of Figure 6a is the increase of the initial elastic modulus $G_0(\gamma)$ with increasing deformations (strain hardening). The response deviates from the linear function $G(t,\gamma<\gamma_{lin})$ at $\gamma \sim 0.5$, yielding for the linear limit $\gamma_{lin} = 0.4 \pm 0.1$. Up to a deformation of 1.75, the time dependence of $G(t,\gamma)$ appears to be rather similar. Actually, we can show that the stress relaxation function for $\gamma < 2$ can be adequately fitted by the stretched exponential

$$G(t,\gamma>\gamma_{lin}) = G_0(\gamma) \exp\left[-\left(\frac{t}{\tau(\gamma)}\right)^{\alpha}\right] \qquad (6)$$

with the fixed stretched exponent of $\alpha = 0.8 \pm 0.02$. The relaxation is thus very comparable to that of the linear regime (eq 4), but here, we explicitly assume some dependencies for the viscoelastic parameters $G_0(\gamma)$ and $\tau(\gamma)$ upon strain.

In a third regime, when the deformation initially applied exceeds 2 (Figure 6b), the overall relaxation

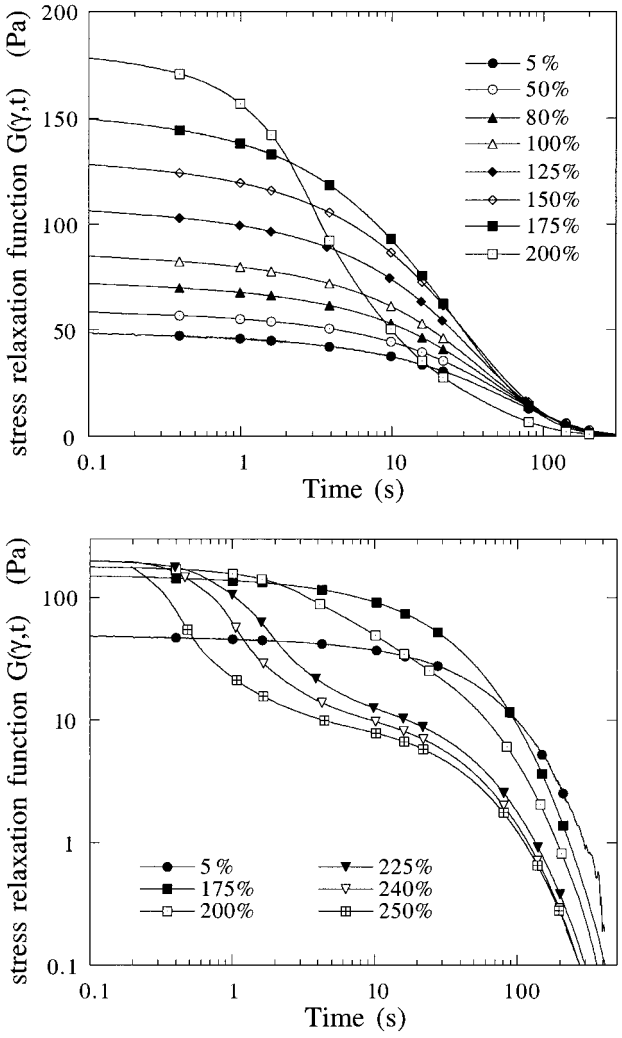

Figure 6. Stress relaxation functions $G(t,\gamma)$ for the F-HEUR/D_2O solution at $\phi = 4\%$ for strain amplitudes γ ranging from 0.05 to 2 (a, top) and from 1.75 to 2.5 (b, bottom) at ambient temperature (T = 20 °C). Note in (b) the use of a double-logarithmic scale. The response deviates from the linear function $G(t,\gamma<\gamma_{lin})$ at $\gamma_{lin} = 0.4 \pm 0.1$.

becomes faster. Around 2.4, $G(t,\gamma)$ exhibits a two-step relaxation. One relaxation is fast and takes few seconds whereas the second occurs in time scales comparable to τ_0. As can be seen from the spectra at 2.25−2.5, most of the initial stress is relaxed in the first fast process. In this high-deformation regime, $G(t,\gamma)$ can be approximated by the sum of two functions: one mono-exponential decay for the rapid initial decrease and one of the form of eq 5 (stretched exponential with $\alpha \sim 0.7$) for the long-time tail.

The elastic modulus $G_0(\gamma)$ extrapolated at $t \rightarrow 0$ and the relaxation time $\tau(\gamma)$ are shown as a function of the applied strain in Figure 7 and Figure 8, respectively. Except at high deformations, the viscoelastic parameters are deduced from fitting the stress relaxations in Figures 6 using eq 6 ($\alpha = 0.8$). For γ above 2, the first time of the two-step relaxation has been considered. Figure 7 exhibits the strain hardening effect of a network of flowers. Above the linear regime ($\gamma_{lin} = 0.4$), the elastic modulus increases with deformation by a factor of 4. Simultaneously, the viscoelastic time $\tau(\gamma)$ decreases by a factor of ~10, with a clear discontinuity at 2. The strain hardening and the reduction of the relaxation time at high strains are the main experimental findings of the present paper. In the next section, we argue about the microscopic mechanisms at the origin of these two effects. On the deformation scale, three regimes will be distinguished: 1, the linear regime ($\gamma < \gamma_{lin} = 0.4$); 2, the strain hardening ($\gamma_{lin} < \gamma < \gamma_{IB} = 2$); and 3, the regime of instantaneous breaking ($\gamma > \gamma_{IB}$).

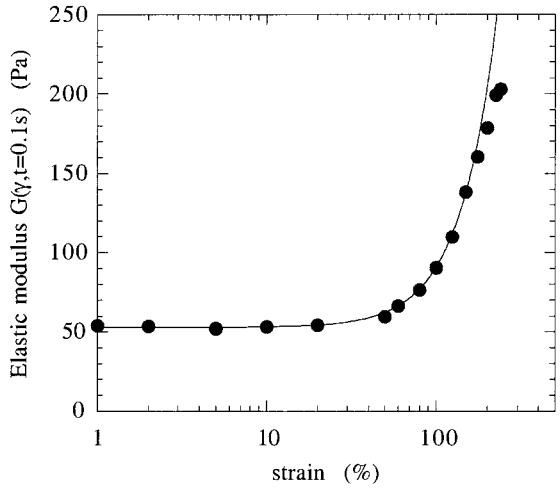

Figure 7. Variation of the elastic modulus $G_0(\gamma)$ extrapolated to $t \rightarrow 0$ as a function of the applied strain γ. Except at high deformations ($\gamma > 2$), $G_0(\gamma)$ is deduced from fitting the stress relaxations in Figure 6a using eq 6 ($\alpha = 0.8$).

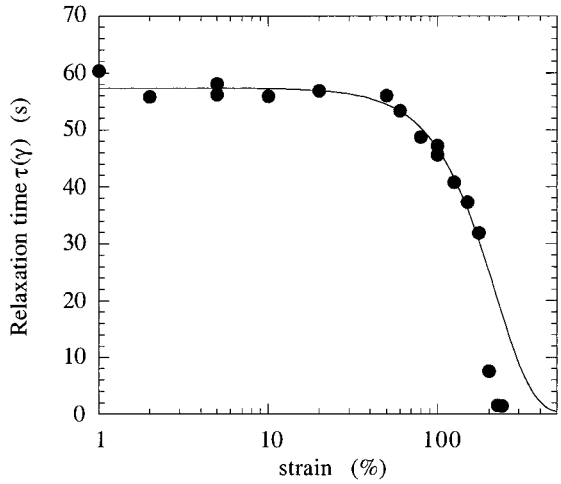

Figure 8. Variation of the viscoelastic relaxation time $\tau(\gamma)$ as a function of the applied strain. Except at high deformations ($\gamma > 2$), $\tau(\gamma)$ is deduced from fitting the stress relaxations in Figure 6a using eq 6 ($\alpha = 0.8$). For γ above 2, the first time of the two-step relaxation has been considered. Three regimes in deformation are discussed in the text: 1, the linear regime ($\gamma < \gamma_{lin} = 0.4$); 2, the strain hardening ($\gamma_{lin} < \gamma < \gamma_{IB} = 2$); and 3, the regime of instantaneous breaking ($\gamma > \gamma_{IB}$).

Discussion

Linear Regime. In our previous investigations of perfluorinated telechelics,[4,9] we have found that the rheological properties obtained in the linear regime of deformation are fitting the mechanical features of a transient network: a sharp increase of the static viscosity above the threshold ϕ^* (~ 1%), a stress relaxation function of Maxwell type (Figure 4), and a relaxation time that is thermally activated (Figure 5). The major differences compared to conventional water-soluble telechelics of HEUR-type are the strongly hydrophobic

fluorinated end caps that favor self-assembling into large clusters ($p \sim 50$).

The transition between the low concentrated sols ($\phi < \phi^*$) and the highly viscoelastic gels ($\phi > \phi^*$) can be described in terms of a percolation transition of bonds. According to percolation theory, the bond percolation threshold for face-centered-cubic symmetry is $p_b = 0.119$.[29] This is a rather weak value, which can also be deduced from simple geometrical arguments. Let us consider one elementary cube of an fcc lattice. Here each corner and each center of faces are occupied by a flowerlike micelle. Within this elementary volume, one counts four particles and 24 possible bonds between neighboring lattice sites. A simple argument consists of saying that bond percolation will occur macroscopically if one can link in a minimal path two flowers located at opposite corners of the cube. This minimum path is three bonds, and thus the overall structure should percolate at the threshold 3/24, a value close to $p_b = 0.119$. Thus, above the percolation threshold, the ratio between the number density of links (or junctions) ν_{link} with respect to the number density of particles n should be such that

$$\nu_{link}/n > 24/4p_b = 0.714 \tag{7}$$

From the value of the elastic modulus in the linear regime ($G_0 = 52$ Pa), the density of elastically active chains is estimated, using the relation

$$G_0 = \nu_{link} k_B T \tag{8}$$

Equation 8 explicitly assumes that the origin of the network elasticity is rubberlike.[30] Using $G_0 = 52$ Pa, one gets a density of links $\nu_{link} = 1.2 \times 10^{16}$ cm^{-3}. On the other hand, from an aggregation number of $p = 50$ (number of telechelic chains per flower) the number of particles in the F-HEUR solution at $\phi = 4\%$ can be derived. One finds $n = 4.2 \times 10^{16}$ cm^{-3},[31] and thus for the ratio $\nu_{link}/n \sim 0.3 < 6p_b$.

This apparent contradiction has been already reported from experiments on HEUR's[5,10] as well as in off-lattice simulations.[32] This inconsistency was solved by postulating the existence of "superbridges" within the network. The "superbridges" are usually described as garlands of flowers that connect two colloids away from each other by more than the nearest-neighbor distance d. In this scheme, the whole garland counts for one unique link. Through the relation

$$D \sim \left(\frac{k_B T}{G_0}\right)^{1/3} \tag{9}$$

an average length scale D for the links that are elastically active can be defined. For the F-HEUR solution at $\phi = 4\%$ investigated here, the prefactor in the previous expression cannot be easily determined since it depends on the actual network connectivity (which is not known). From the percolation threshold, a minimum value for D can be derived: $D > 620$ Å. In conclusion of this first subsection, we will say that the perfluorinated telechelics are building a temporary network of flowers; however, even at a concentration $\phi = 4\%$, the "lattice parameter" D of the elastic network seen by rheology is larger than the average distance between flowers.

Nonlinear Regime. The first mechanism to be described is the one responsible for the strain hardening. At large deformations, the network obviously becomes stiffer. According to eq 8, the increase of $G_0(\gamma)$ observed in Figure 7 could be due to an increase of the number of elastically active chains ν_{link}. However, in step-strain experiments, the deformation is imposed within a time interval of $\Delta t = 50$ ms, which is 3 decades below the internal material time τ_0. It is thus rather improbable that the increase in $G_0(\gamma)$ could be due to an instantaneous (on the time scale of τ_0) rise in the density of links. A much more plausible assumption is to ascribe the strain hardening to the nonlinear mechanical response of the polymeric chains subjected to high extensions. Assuming an affine deformation γ, a chain perpendicular to the vorticity plane and of extension r_0 in the undeformed state will be extended at a value $r(\gamma) = r_0(1 + \gamma^2)^{1/2}$. From neutron scattering, we found for the F-HEUR solution at $\phi = 4\%$ a nearest-neighbor distances $d \sim 300$ Å. Taking for the fully extended PEO chain with 227 monomers ($M_n = 10\,000$ g/mol) a value of $L = 800$ Å, one gets $r_0 = 0.27$ (the core of the micellar flowers has been taken into account). As a result, the linear strain limit $\gamma_{lin} = 0.4$ and the instantaneous breaking strain $\gamma_{IB} = 2$ corresponds to chain extensions $r = 0.3$ and $r = 0.6$, respectively. Because the strain hardening regime corresponds to the nonlinear regime of chain extension,[30] we conclude that the increase of elasticity of the network under deformation is related to the increase of stiffness of the active links. Note that, under the assumption of affine deformation, the previous reasoning is also applicable if the elastically active chains are "superbridges".

The second fundamental property of the fluorinated telechelic networks is the decrease of the relaxation time $\tau(\gamma)$ at large deformations. We interpret this decrease as the evidence that the disengagement probability of an end cap from a junction point depends on the tension exerted by the polymeric chain. This idea was first suggested by Yamamoto 40 years ago[14] and has been reexamined by Tanaka and Edwards[12,13] and by Marruccci et al.[19] Recently, Tam et al.[10] have reported experiments using the superposition of oscillations on steady shear measurements on a 2.0 wt % HEUR polymer solution. These authors have found a reduction of the average relaxation time in the shear-thickening regime (which furthermore coincides with the hardening of the network) that they ascribe to the increase of the breakage probability with the stretching of the chains.

The regime of instantaneous breaking observed at deformations $\gamma > 2$ and characterized by a two-step relaxation function is also of interest (Figure 6b). It is possible that these two steps reflect two populations of elastically active chains. The first population detaches from the network rapidly after the inception of the strain. Because the chains are highly stretched, the elastic energy associated then compares with the activation barrier for disengagement of the end caps. This instantaneous disruption of the network results in a fast decrease of the stress. On the other hand, the second relaxation concerns the less stretched chains, which then relax within the typical network time and according to the linear response function (eq 5).

Conclusion

We have investigated the nonlinear mechanical responses of a transient network made of flowerlike micelles. These flowers result from the self-assembling of perfluoroalkyl telechelics (F-HEUR). On a F-HEUR

solution at $\phi = 4\%$, step-strain experiments of amplitudes γ comprised between 0.05 and 2.5 reveal two fundamental results. With increasing γ, we observe the strain hardening of the elastic modulus $G_0(\gamma)$ and, simultaneously, the decrease of the viscoelastic relaxation time $\tau(\gamma)$. These findings are interpreted in terms of nonlinear stretching of the elastically active chains. Using the structural data obtained by small-angle neutron scattering, we show that the strain hardening regime ($0.4 < \gamma < 2$) fits rather well the regime of nonlinear chain extensions. We conclude that the increase of network elasticity at large strains is related to the increase of stiffness of the active links (and not their number density). On the other hand, the decrease of the relaxation time $\tau(\gamma)$ at large deformations is viewed as the evidence that the chain breakage probability depends on the chain extension (or end-to-end distance).[14]

In this paper we have discussed only one set of data that was obtained at one temperature ($T = 20$ °C) and one concentration ($\phi = 4\%$). However, one has to keep in mind that the strain hardening and the decrease of the relaxation time at large deformations (results of Figures 7 and 8, respectively) are representative of a class of materials, namely the water-soluble telechelics with perfluorinated end caps. We have recently performed the same kinds of experiments as those depicted in the present paper on perfluoroalkyl telechelics by changing (i) the nature of the spacer between the hydrophobes and the chain, (ii) the length of the middle chain, (iii) the temperature, and (iv) the telechelic concentration (being always above the percolation transition). In all these experiments,[20] we have found an increase of the elastic modulus and a decrease of the relaxation time, the same results as those displayed in Figures 7 and 8.

Finally, we do believe that the microscopic mechanisms revealed by the step-strain experiments will also be relevant in the steady shear properties of transient networks, as for instance in the shear thickening and shear thinning regimes mentioned in the Introduction.

Acknowledgment. The authors thank M. Adam, A. Ajdari, F. Molino, J.-F. Palierne, and G. Porte for fruitful discussions. We are also grateful to R. Aznar, D. Calvet, M. Viguier, and A. Collet for the synthesis of the telechelic polymers. Y.S. and J.-F.B. acknowledge the financial and experimental support from the Laue-Langevin Institute during the course of the neutron experiments. The present work is partly funded by the European Community (Contract FMRX-CT96-003).

References and Notes

(1) Winnik, M. A.; Yekta, A. *Curr. Opin. Colloid Interface Sci.* **1997**, *2*, 424.
(2) Gast, A. P. *Langmuir* **1996**, *12*, 2, 4060.
(3) Semenov, A. N.; Joanny, J.-F.; Khokhlov, A. R. *Macromolecules* **1995**, *28*, 1066.
(4) Séréro, Y.; Aznar, R.; Porte, G.; Berret, J.-F.; Calvet, D.; Collet, A.; Viguier, M. *Phys. Rev. Lett.* **1998**, *81*, 5584.
(5) Annable, T.; Buscall, R.; Ettelaie, R.; Whittlestone, D. *J. Rheol.* **1993**, *37*, 695.
(6) Xu, B.; Yekta, A.; Li, L.; Masoumi, Z.; Winnik, M. A. *Colloids Surf. A: Physiochem. Eng. Aspects* **1996**, *112*, 239.
(7) Amis, E. J.; Hu, N.; Seery, T. A. P.; Hogen-Esch, T. E.; Yassini, M.; Hwang, F. *Adv. Chem. Ser.* **1996**, *248*, 279.
(8) Xu, B.; Li, L.; Yekta, A.; Masoumi, Z.; Kanagalingam, S.; Winnik, M. A.; Zhang, K.; Macdonald, P.; Menchen, S. *Langmuir* **1997**, *13*, 3, 2447.
(9) Cathébras, N.; Collet, A.; Viguier, M.; Berret, J.-F. *Macromolecules* **1998**, *31*, 1305.
(10) Tam, K. C.; Jenkins, R. D.; Winnik, M. A.; Bassett, D. R. *Macromolecules* **1998**, *31*, 4149.
(11) Green, M. S.; Tobolsky, A. V. *J. Chem. Phys.* **1946**, *14*, 80.
(12) Tanaka, F.; Edwards, S. F. *Macromolecules* **1992**, *25*, 5, 1516.
(13) Tanaka, F.; Edwards, S. F. *J. Non-Newtonian Fluid Mech.* **1992**, *43*, 247.
(14) Yamamoto, M. *J. Phys. Soc. Jpn.* **1956**, *11*, 413; **1957**, *2*, 1148; **1958**, *13*, 1200.
(15) Lodge, A. S. *Rheol. Acta* **1968**, *7*, 379.
(16) Otsubo, Y. *Langmuir* **1999**, *15*, 1960.
(17) Witten, T. A. *J. Phys. (Paris)* **1988**, *49*, 1055.
(18) Vrahopoulou, E. P.; McHugh, A. J. *J. Rheol.* **1987**, *31*, 371.
(19) Marrucci, G.; Bhargava, S.; Cooper, S. L. *Macromolecules* **1993**, *26*, 6483.
(20) Calvet, D.; Viguier, M.; Collet, A.; Séréro, Y.; Berret, J.-F., manuscript in preparation.
(21) Grest, G. S.; Fetters, L. J.; Huang, J. S. *Adv. Chem. Phys.* **1996**, *19*, 67.
(22) Daoud, M.; Cotton, J.-P. *J. Phys. (Paris)* **1982**, *43*, 531.
(23) Pedersen, J. S.; Gerstenberg, M. C. *Macromolecules* **1996**, *29*, 9, 1363.
(24) Adam, M.; Lairez, D. *Fractals* **1993**, *1*, 149. Förster, S.; Wenz, E.; Lindner, P. *Phys. Rev. Lett.* **1996**, *77*, 95.
(25) Cotton, J.-P. In *Diffusion des Neutrons aux Petits-Angles;* Cotton, J.-P., Nallet, F., Eds.; EDP Sciences: Albé, Massif Vosgien, France, 1998; Vol. 9, pp 21−49.
(26) Raspaud, E.; Lairez, D.; Adam, M. *Macromolecules* **1996**, *29*, 9, 1269.
(27) Pham, Q. T.; Russel, W. B.; Thibeault, J. C.; Lau, W. *Macromolecules* **1999**, *32*, 2996.
(28) Alami, E.; Rawiso, M.; Isel, F.; Beinert, G.; Binana-Limbele, W.; François, J. *Adv. Chem. Ser.* **1996**, *248*, 343.
(29) Stauffer, D.; Aharony, A. *Introduction to Percolation Theory*, 2nd ed.; Taylor and Francis: London, 1994.
(30) Larson R. G. *Constitutive Equations for Polymer Melts and Solutions;* Butterworths: Boston, 1988.
(31) This value is slightly lower than the one derived from the position of the first oscillation of the structure factor. The difference between both determinations arises from the different aggregation numbers found in the dilute regime and in the viscoelastic regime. For the present argument, this difference is not crucial.
(32) Groot, R. D.; Agterof, G. M. *Macromolecules* **1995**, *28*, 8, 6284.

MA991349D